Tunable Spin-Superconductor Coupling of Spin 1/2 Vanadyl Phthalocyanine Molecules

Available as *Nano Lett.* 2018, 18, 12, 7955–7961 https://doi.org/10.1021/acs.nanolett.8b03921

Tunable spin-superconductor coupling of spin ½ vanadyl-phthalocyanine molecules

Luigi Malavolti,[*, †§‡] *Matteo Briganti,*[¥] *Max Hänze,*[†§‡] *Giulia Serrano,*[¥] *Irene Cimatti,*[¥] *Gregory McMurtrie,*[†§‡] *Edwige Otero,*[^] *Philippe Ohresser,*[^] *Federico Totti,*[¥] *Matteo Mannini,*[¥] *Roberta Sessoli,*[¥] *and Sebastian Loth*[*, †§‡]

[†] Institute for Functional Matter and Quantum Technologies, University of Stuttgart, 70569 Stuttgart, Germany

[§] Max Planck Institute for the Structure and Dynamics of Matter, 22761 Hamburg, Germany

[‡] Max Planck Institute for Solid State Research, 70569 Stuttgart, Germany

[¥] Dipartimento di Chimica "Ugo Schiff" & INSTM RU, Università degli Studi di Firenze, Via della Lastruccia 3-13, 150019 Sesto Fiorentino (Firenze), Italy

[^] Synchrotron SOLEIL, 4891192 Gif-sur-Yvette, France

KEYWORDS:

Yu-Shiba-Rusinov bound states, molecular magnetism, superconductivity, X-ray magnetic circular dichroism, Scanning Tunneling Spectroscopy, Density functional theory

Available as *Nano Lett.* 2018, 18, 12, 7955–7961 https://doi.org/10.1021/acs.nanolett.8b03921

ABSTRACT:

Atomic-scale magnetic moments in contact with superconductors host rich physics based on the emergence of Yu-Shiba-Rusinov (YSR) magnetic bound states within the superconducting condensate. Here we focus on a magnetic bound state induced into Pb nanoislands by individual vanadyl-phthalocyanine (VOPc) molecules deposited onto the Pb surface. The VOPc molecule is characterized by a spin magnitude of ½ arising from a well-isolated singly-occupied d_{xy} orbital and is a promising candidate for a molecular spin qubit with long coherence times. X-ray magnetic circular dichroism (XMCD) measurements show that the molecular spin remains unperturbed even for molecules directly deposited on the Pb surface. Scanning tunneling spectroscopy and density functional theory (DFT) calculations identify two adsorption geometries for this "asymmetric" molecule (i.e. absence of a horizontal symmetry plane): a) oxygen pointing towards the vacuum and the Pc laying on the Pb, showing negligible spin-superconductor interaction, and b) oxygen pointing toward the Pb, presenting an efficient interaction with the Pb and promoting a Yu-Shiba-Rusinov bound state. Additionally, we find that in the first case a YSR state can be induced smoothly by exerting mechanical force on the molecules with the STM (scanning tunneling microscope) tip. This allows the interaction strength to be tuned continuously from an isolated molecular spin case, through the quantum critical point (where bound state energy is 0) and beyond. DFT indicates that a gradual bending of the VO bond relative to the Pc ligand plane promoted by the STM tip can modify the interaction in a continuously tunable manner. The ability to induce a tunable YSR state in the superconductor suggests the possibility of introducing coupled spins on superconductors with switchable interaction.

TEXT:

Available as *Nano Lett.* 2018, 18, 12, 7955–7961 https://doi.org/10.1021/acs.nanolett.8b03921

Magnetic nano-objects in close proximity to superconductors have been proposed as possible platforms for quantum computing, examples include entangled spin-photon states for ensembles of magnetic moments in superconducting resonators[1–5] as well as topological states of coupled magnetic moments.[6–9] The interaction strength of the magnetic moment with the superconducting phase is a key parameter when it comes to defining the physical properties of the system. While a decoupled system is desirable for the realization of spin-photon states,[1–5] finite coupling between the magnetic moment and the superconducting phase is necessary in order to utilize many-body states such as Majorana edge modes at the ends of magnetic chains.[6–11]

The coupling between a paramagnetic impurity and a superconducting surface imposes a spin-dependent scattering potential that locally perturbs the superconducting condensate and effectively lowers the energy needed to break Cooper pairs. Locally, this gives rise to the formation of a magnetic Yu-Shiba-Rusinov (YSR) bound state that appears as quasiparticle excitations within the superconducting gap.[12–14] For weak coupling the superconducting condensate remains composed entirely of paired electrons. When the bound state energy is 0 a quantum phase transition[15] occurs and the ground state contains localized quasiparticles that screen the magnetic moment of the impurity[16] (see Figure 1a). Systems in both energy regimes have been reported for several species of magnetic atoms[17–20] and molecules[15,21–24] on different superconducting surfaces.

YSR states are observed in a scanning tunneling spectroscopy experiment as pairs of conductance peaks inside the superconducting gap (Δ_0), positioned symmetrically with respect to zero bias. The impurity's magnetic moment, orbital configuration[25] and orbital overlap[26] with the surface are important parameters, which alter the YSR states,[27] yet these properties remain elusive as STM measurements are typically insensitive to them. Notably, while the majority of experimental work has been focused on magnetic impurities with large magnetic moments and

significant magnetic anisotropy,[15,17–23] theoretical reports mostly address spin ½ isotropic impurities.[12–14,28] Whereas magnetic atoms adsorbed directly onto a superconducting surface typically interact strongly, magnetic molecules offer tunability of this interaction via design flexibility of the ligand shell.[21,22] The use of flat paramagnetic metal-organic molecules, such as metal phthalocyanines (MPc), as spin carriers is particularly interesting. The non-covalent interaction with the substrate is mediated through the organic ligands, forming a very robust interface. At the same time, important parameters affecting the coupling with superconductors vary with the number and direction of the singly occupied orbitals (the magnetic orbitals) characterizing the metal ion coordinated by the organic ligand. In the series of MPc molecules, S=1/2 systems have recently attracted a great deal of interest as potential qubits due to their long spin coherence time[29] and addressability via electromagnetic radiation pulses. In particular, the "asymmetric" vanadyl-phthalocyanine, VOPc, molecule exhibits room temperature quantum coherence thanks to its coordination rigidity and an almost negligible orbital contribution, confirmed by a *g* factor very close to 2.[29] Moreover, a remarkable coupling with photons in a superconducting cavity suggests the possibility of including VOPc in quantum circuits.[30] The vanadyl unit is also present in a weakly interacting dimer acting as a quantum logic gate and proposed for quantum simulation.[31]

In this letter, we deposit vanadyl phthalocyanine (VOPc) molecules onto a Pb(111) superconducting surface (see Figure 1b). The crucial question of how the VOPc's spin ½ is modified upon adsorption onto a superconductor is addressed. A superconductor was chosen because the superconducting gap was reported to affect spin lifetimes less than metallic surfaces.[21] Here, the chemical stability of the molecule on the Pb surface is established by X-ray photoelectron spectroscopy (XPS) and the persistence of the molecular spin ½ on the superconducting surface is

confirmed by X-ray magnetic circular dichroism (XMCD). Scanning tunneling microscopy, in combination DFT calculations, finds two different absorption geometries for the VOPc molecules on the Pb surface. These molecules can lie down on the Pb surface with the phthalocyanine ligand exposing the oxygen of the vanadyl towards vacuum (labeled *oxygen-up* molecule throughout the text) or with the oxygen of the vanadyl towards the Pb (labeled *oxygen-down* molecule), analogously to what was reported for other surfaces.[32–34] The *oxygen-up* molecules show negligible spin-superconductor interaction, whereas *oxygen-down* molecules have sufficient interaction to induce a Yu-Shiba-Rusinov bound state. We find that on *oxygen-up* molecules a YSR bound state can be smoothly induced by moving the STM tip towards the molecule and exerting mechanical force onto the VO center. Detailed DFT analysis identifies a tilt of the V=O bond toward the phthalocyanine ligand as a probable mechanism for the smooth increase in interaction strength seen in STM measurements. These results open up the possibility of achieving a switchable spin-superconductor interaction, of great relevance in quantum information technology based on spins coupled through a superconductor.[5,35]

The experiments were carried out on two different samples: a monolayer film of VOPc on a Pb (111) single crystal - optimal for the spatially averaging X-ray measurements - and individual VOPc molecules on ultrathin Pb nano-islands grown on Si(111)-7x7,[36] optimized for our low-temperature scanning tunneling spectroscopy investigation (Figure 1b). Both samples expose a (111) surface of Pb onto which the molecules were deposited, ensuring a comparable environment (see Supporting Information for further details on both preparation methods). The single crystal was used to establish the structural and magnetic integrity of the VOPc system on the Pb (111) surface by combining XPS, XMCD and variable-temperature STM. The Pb nano-islands provide a distinct advantage for the characterization of the spin-superconductor coupling via spectroscopy

of the YSR state. The nanoscale spatial confinement of the Pb islands[37] allows the film to remain superconducting up to high magnetic field, thereby suppressing the coherence peaks which may otherwise overshadow a weakly bound YSR state close to the gap edge.

Individual VOPc molecules deposited on Pb islands appear as four-lobed objects of approximately 1.5 nm diameter, mirroring the *four-fold* symmetry of the phthalocyanine ligand (Figure1b inset and Figure 2a). We observe two types of STM topographies for the VOPc molecules: some showing a protrusion in the center of the four-lobed structure and others showing no central feature, Figure 2a. We attribute these two contrasts to two adducts of VOPc on the Pb surface, one with phthalocyanine binding to Pb (*oxygen-up*) and one with oxygen binding to Pb (*oxygen-down*).[32–34] To gain more insight into the electronic structure and the energetics involved in the adsorption we performed periodic mixed Gaussian and plane-wave *ab initio* density functional theory calculations (see also Supporting Information). Calculated STM images for both adducts match well with the measured images and assign the *oxygen-up* configuration to the image with the central protrusion (Figure 2b) and the *oxygen-down* configuration to the flat four-lobed image (Figure 2c). In the *oxygen-up* configuration the interaction with the surface is mediated through the π-system of the Pc whereas the oxygen atom of the vanadyl group participates significantly in the binding for the *oxygen-down* configuration. Surprisingly, in their most stable adsorption sites, both adducts have very similar binding energies of -5.77 eV (-133.0 kcal/mol) for *oxygen-up* and -5.83 eV (-134.527 kcal/mol) for *oxygen-down*. Other possible adsorption sites are also close in energy, within 0.03 eV (0.7 kcal/mol) for *oxygen-up* and 0.16 eV (3.7 kcal/mol) for *oxygen-down* (see Table S1). This result matches well to the experimental observation that both adsorption geometries are found with approximately equal probability. The presence of both

oxygen-down and *oxygen-up* molecules on the Pb surface is further corroborated by the presence of two main components in the O*1s*, V*2p*$_{3/2}$ and N*1s* regions[32] observed in the XPS spectra (see Figure S3).

The robustness of the magnetic moment of VOPc on Pb was verified by XMCD experiments carried out at the DEIMOS beamline (SOLEIL synchrotron, France). Prior to this, the orientation of the VOPc layer on Pb was confirmed to be the same as in the STM experiments by X-ray natural linear dichroism, XNLD, measurements at the $L_{2,3}$ vanadium edges (Figure S4). The molecules' magnetic response was probed by recording X-ray absorption spectra (XAS) at the $L_{2,3}$ vanadium edges using left and right circularly polarized light in a magnetic field of 6 T parallel to the X-ray beam propagation at 4.2 K (Figure S5) and 2 K temperature Figure 1c. The presence of the magnetic field quenches the superconducting phase. The XMCD spectrum was obtained as $(\sigma^+ - \sigma^-)$ where σ^+ (σ^-) is the absorption X-ray cross section for the helicity pointing to (opposite to) the photon propagation. The XAS spectrum shows a structured shape at the vanadium L_3 edge and a broader asymmetric L_2 edge. The oxygen K-edge dominates the spectrum above 530 eV. Previous studies of VOPc on iron, cobalt, nickel,[38] silver and silicon[32] showed less-structured XAS but are consistent with the higher energy-resolution findings obtained here. The relative dichroism (XMCD%) reaches its maximum magnitude at 518 eV photon energy, of -40 % at 4.2 K and -51 % at 2 K. A small, but significant, dichroic signal is also observed at the oxygen K-edge (see inset Figure 1c). This shows that VOPc remains magnetic upon adsorption onto Pb.

In bulk, VOPc is in a $3d^1$ configuration and the magnetic moment of 1 Bohr magneton stems from the spin of the single electron in the d shell.[29] The persistence of this spin ½ on the Pb surface can be evaluated by recording the XMCD% signal evolution while sweeping the magnetic field

from -6 T to 6 T at 2 K and 4.2 K temperature. This is an alternative approach, as the proximity of the L_2 and L_3 edges makes XMCD sum rules analysis uncertain.[32] The signal obtained can be considered proportional to the magnetization of the system and its field dependence is in very good agreement with the expected behavior for a ½ spin system (Figure 1d and Supporting Information). Furthermore, a thick-film reference sample, prepared by drop-casting a VOPc 1 mM solution in dichloromethane onto gold on mica, showed an XMCD signal very similar to that of the monolayer sample (see Figure S6). Small differences can be related to the expected absence of preferential orientation in the thick film. This confirms that VOPc molecules retain their spin ½ on the Pb surface.

To quantify the coupling between the VOPc spin and the superconductor we use an STM at 0.5 K to measure differential conductivity spectra, dI/dV(V), of individual VOPc molecules on Pb nano-islands. A normal-conducting metal tip was used for this characterization to prevent the possibility of a YSR state developing due to the proximity of a superconducting tip.[24] A magnetic field of 0.1 T parallel to the surface was applied to reduce the magnitude of the coherence peaks. We find that dI/dV(V) spectra acquired on individual *oxygen-up* and *oxygen-down* molecules differ significantly (Figure 2d,e). The *oxygen-down* molecule shows two pronounced peaks within the superconducting gap of the Pb island at $|E_b/e| = 0.25$ mV bias, whereas the *oxygen-up* molecule shows just the superconducting gap of Pb and no in-gap features. The two peaks of the *oxygen-down* molecule match to the electron- and hole-like excitations of a YSR state[28] that appears upon coupling of a local magnetic moment to the superconducting condensate of the Pb nano-island. Similar YSR states have been observed for other types of metal-phthalocyanines.[22,23] The coherence peaks of the superconducting substrate are readily observed in the spectrum of the *oxygen-up* molecule while they are suppressed for the *oxygen-down* molecule. Outside the

superconducting gap, no spectral features related to the presence of a spin excitation or a Kondo peak were observed for both molecular orientations. The majority of investigated molecules (16 out of 19) match to this bimodal behavior, indicating strongly orientation-dependent spin-superconductor coupling between the spin ½ of the VOPc and the Pb surface. In the *oxygen-down* orientation the spin appears to be coupled strongly to the superconductor, whereas the molecular spin is decoupled for the *oxygen-up* orientation.

Considering that the molecular spin mainly resides on the vanadium atom, it is remarkable to find no YSR state for *oxygen-up* molecules where, according to DFT, the vanadium atom is 0.35 Å closer to the Pb surface. This suggests that the oxygen atom mediates the molecule-Pb interaction. ~~, as also pointed out by XPS results~~

The coupling mechanism between the unpaired electrons of the VOPc and the superconducting surface can be elucidated by DFT as expected to be comparable to the amount the VOPc spin delocalizes on the normal-conducting Pb surface. We find that the unpaired electron on the V atom remains practically unperturbed in the *oxygen-up* configuration. It shows negligible spin delocalization into the first layer of the Pb surface (< 0.002 electrons, calculated as the Mulliken spin density, see Table 1). In contrast, *oxygen-down* molecules show a much stronger delocalization (up to 0.025 electrons, see Table 1).

In order to gauge whether the calculated spin delocalization provides sufficient spin-superconductor coupling for the formation of a YSR state, we performed the same calculation for a known system: manganese(II) phthalocyanine (MnPc) molecules on Pb(111). They were reported to exhibit YSR bound states in the strong coupling regime.[22] We find spin delocalization into the Pb surface of 0.23, 0.11 and 0.11 electrons for Mn located on the top, bridge and hollow

sites of Pb(111), respectively (see also Table S3). The variation found among the adsorption sites agrees with the experimental findings reported by ref.[22] Furthermore, after accounting for MnPc having up to five singly-occupied d-orbitals instead of one, the spin delocalization is comparable to that of *oxygen-down* VOPc. As such, our calculation predicts the observation of a YSR state for *oxygen-down* VOPc and is consistent with the absence of a YSR state on *oxygen-up* VOPc.

Thus, the *oxygen-up* VOPc exhibits the unique property of being a magnetic molecule in electrical contact with the Pb surface with a spin that is decoupled from the superconductor. Controllably inducing coupling would give us the opportunity to study the emergence of the YSR state. The STM tip provides such a means of perturbation; it is known to manipulate the properties of atoms and molecules on surfaces[21,39–43] and has recently been applied to tune correlated phenomena such as Kondo resonance,[44] as well as to modify the binding energy of YSR states.[27]

Here, we exploit the effect of mechanical force exerted by the STM tip on the *oxygen-up* VOPc molecules to promote the emergence of a YSR bound state. We find that a YSR state emerges when the tip is very close, i.e., the mechanical interaction is significant. Since we are close to point-contact (0.1-0.3 G_o) estimates from literature place the force in the 10's of nN range.[45] dI/dV(V) spectra of *oxygen-up* VOPc molecules are acquired while progressively reducing the tip-sample distance, (Figure 3a). At large tip-sample distances dI/dV(V) spectra show only a gap and do not vary with tip movement. The $\Delta Z = 0$ reference was chosen in this regime, at a junction setpoint

of 1 nA and 5 mV. After a significant approach of the tip (ΔZ = -1.8 Å) two conductance peaks are observed at ±0.43 mV, well separated from the edges of the superconducting gap. These peaks are characteristic of the two quasiparticle excitations of a YSR state.

In order to track the evolution of the YSR state we first fit the superconducting gap spectrum and subsequently add two Lorentzian curves that fit the in-gap peaks (see Supporting Information for details). This yields the bound state energy and peak height as a function of tip movement, Figure 3b. For large tip-sample distances ($\Delta Z > -1.58$ Å) the spectra appear to be unperturbed by the presence of the molecular spin. This indicates that the spin is initially decoupled from the superconductor and no YSR state has formed. The first spectrum for which the fit yields an in-gap state with significant confidence is at $\Delta Z = -1.58$ Å. By approaching the STM tip a YSR state emerges, indicating increased coupling between molecular spin and superconductor. Further approach leads to a gradual reduction of E_b eventually reaching zero energy at $\Delta Z = -2.1$ Å. At this point we observe a sharp transition of the peaks' asymmetry from positive to negative. By approaching the tip even further, $|E_b|$ increases again. This behavior has been attributed to be the signature of a quantum phase transition from the weak to the strong coupling regime[16] indicating that the coupling induced by the tip can become strong enough to localize quasiparticles at the VOPc.

DFT is used to determine how the STM tip induces the observed molecule-superconductor coupling. Due to the chemical stability of the vanadyl, chemical interaction with the tip is unlikely; as such our investigation was focused on mechanical effects. The negligible role of chemical interaction is also suggested by the observation of a smooth and reproducible distance dependence curve. This simplified model allows us to significantly reduce the parameter space and we find that it reproduces the observation well. Surprisingly, a simple compression that approaches the *oxygen-up* complex closer to the surface does not significantly increase the spin delocalization onto the Pb (reaching only 0.004 electrons, Table 2). The vanadium d_{xy} orbital that carries the spin is parallel to the Pb surface even under compression. Thus, direct overlap remains negligible

(Figure 4b). Additionally, the symmetry of the d_{xy} orbital is such that it does not strongly overlap via σ interactions with the coordinated nitrogen orbitals of the Pc ligand, but rather with weak π interactions. This significantly reduces the indirect coupling with the Pb surface through the Pc ligand, observed for instance for CuPc on V,[25] which would increase under compression.

By tilting the VO with respect to the surface normal, the symmetry of the whole system can be lowered and spin delocalization induced. The tilt effectively moves the magnetic orbital out of the Pc plane allowing d_{xy}, d_{xz} and d_{yz} to mix, making the spin delocalization more effective on both the Pc ligand and the Pb surface (Figure 4c). Moreover, the *xy* component is shifted towards the Fermi level, leading to a stronger interaction with the surface (Figure 4d).[22,46] To reach an amount of spin delocalization comparable to that found for *oxygen-down* molecules requires a tilt of approximately 30 ° (Figure 4c). Experimentally, such a tilt can be induced by a tip-molecule interaction acting oblique to the surface. This same interaction is used when displacing VOPc molecules laterally.

In order to rule out the possibility that the YSR state in the *oxygen-down* molecules is also induced by the tip, we studied how the dI/dV(V) spectrum varies as the tip is withdrawn from the molecule (Figure 3c). Notably, the YSR bound state energy and the peak intensity asymmetry remain constant (Figure 3d). DFT calculations corroborate these observations, showing no change in the spin delocalization (Table S4). The peak intensity asymmetry indicates that the *oxygen-down* VOPc molecule is in a strong coupling regime regardless of tip perturbation. A relative increase of the YSR resonance heights is observed, which can be attributed to increasing overlap between the tip and molecule's orbitals boosting the excitation probability of the YSR bound state. As such, we conclude that the YSR state is already present on the unperturbed *oxygen-down* molecules.

Available as *Nano Lett.* 2018, 18, 12, 7955–7961 https://doi.org/10.1021/acs.nanolett.8b03921

This study shows that the VOPc molecule on Pb offers a spin ½ system with full tunability of the spin-superconductor interaction from decoupled to strongly coupled. XMCD measurements confirm that VOPc retains its magnetic moment on the ~~superconducting~~ Pb (111) surface at temperatures below 4.2 K. STM and DFT find that the non-planar VOPc adsorbs in two binding geometries: *oxygen-down* which is strongly coupled to the surface and shows a YSR-state, and *oxygen-up* which is decoupled. Tilting the VO bond toward the Pc plane lowers the molecule's symmetry, smoothly increases spin-superconductor coupling and a fully tunable YSR state emerges. The state can be tuned from the weak coupling regime, to past the quantum phase transition marking strong coupling. This property makes VOPc a viable candidate for exploring coupled states in arrays or chains of molecules. In particular, the VOPc/Pb system provides a promising platform of decoupled molecular spins that are less than one nanometer away from the superconductor and therefore in the extreme near-field. This approach may overcome the challenge of reaching the strong spin-photon coupling limit for molecule-based quantum information processing schemes.

Available as *Nano Lett.* 2018, 18, 12, 7955–7961 https://doi.org/10.1021/acs.nanolett.8b03921

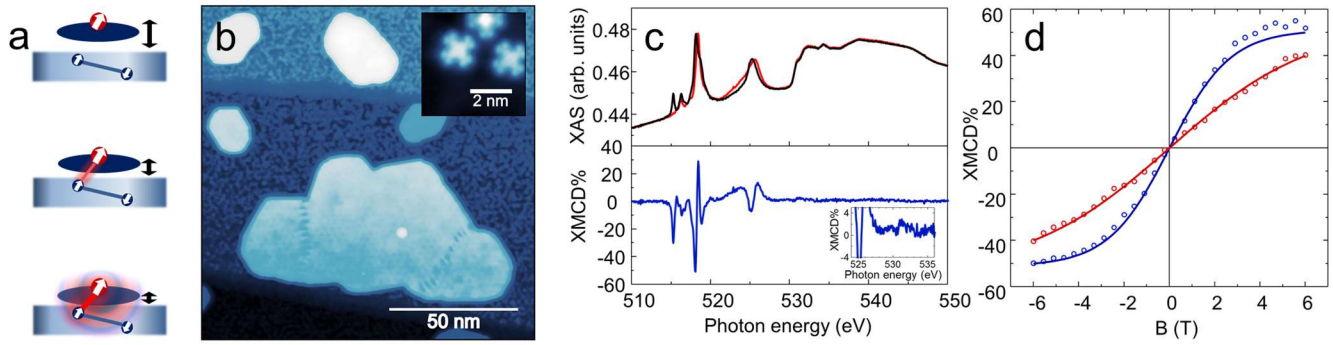

Figure 1. Magnetic signature of VOPc molecules on Pb. (a) Interaction scheme of a molecular magnetic impurity (red circle) with the Cooper pairs of a superconducting surface; the three different coupling regimes are, from top to bottom: decoupled spin, weak interaction (superconductor locally perturbed) and strong interaction (quasiparticle localized at impurity). (b) Large-scale STM image of the Pb nano-islands grown on Si(111)-7x7 (tunnel junction setpoint 2.0 V, 0.1 nA) showing heights between 6 ML and 8 ML, as well as different sizes. Inset: STM image of VOPc molecules on a Pb island (tunnel junction setpoint 1.0V, 0.1nA). (c) Top panel: x-ray absorption spectra, XAS, acquired at the $L_{2,3}$ vanadium edges with circularly polarized light (σ^+ red and σ^- black) of a VOPc monolayer deposited on Pb(111). Bottom panel: x-ray circular magnetic dichroism signal, XMCD ($\sigma^+ - \sigma^-$) recorded at 2 K temperature and 6 T magnetic field. Inset: zoom to XMCD of oxygen K edge. (d) Magnetization curves of VOPc on Pb acquired at 2 K (blue dots) and 4.2 K (red dots) along with expected magnetization curves for a spin ½ with a g value $g = 2$ (solid lines).

Available as *Nano Lett.* 2018, 18, 12, 7955–7961 https://doi.org/10.1021/acs.nanolett.8b03921

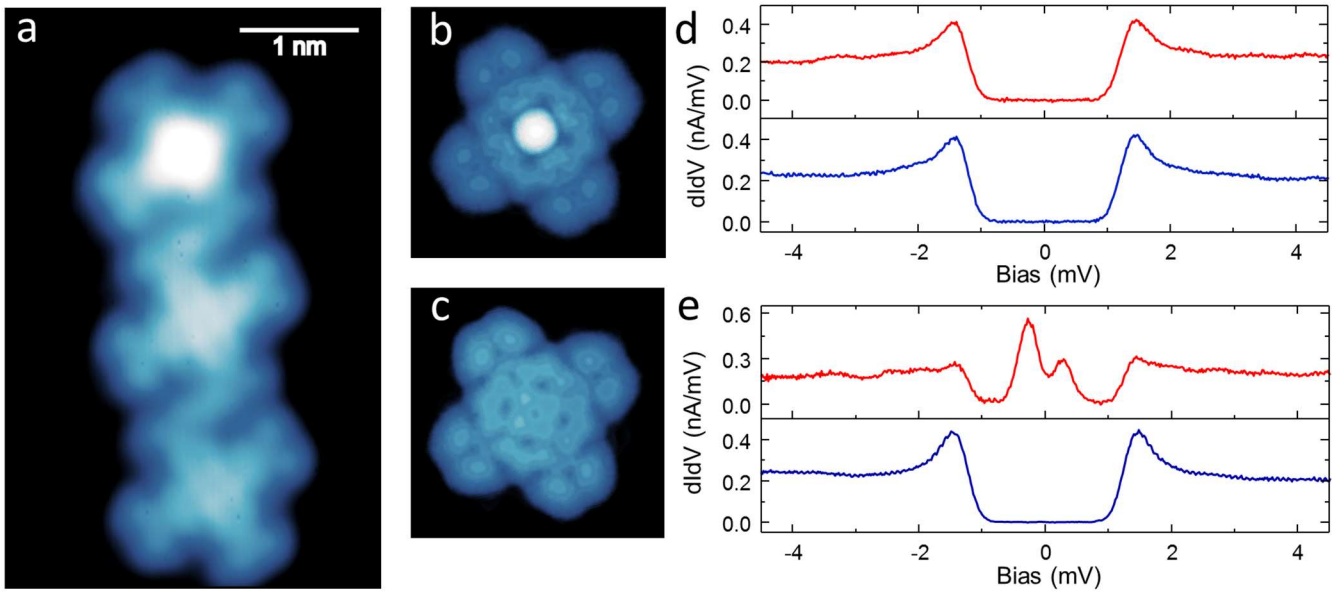

Figure 2. Adsorption geometries and dI/dV(V) spectra of VOPc on Pb. (a) STM image of VOPc molecules on a Pb island (tunnel junction setpoint 1.0 V, 0.1 nA); first molecule from top is in the *oxygen-up* geometry, whereas the other two are in the *oxygen-down* geometry. (b) Calculated STM image for *oxygen-up* and (c) *oxygen-down* geometry at 1.0 V bias; Image scale same as in (a). (d) dI/dV(V) spectrum of an *oxygen-up* molecule (red curve) and spectrum of the bare Pb surface on the same nano-island (blue curve); tunnel junction setpoint 5.0 mV, 1.0 nA, temperature 0.5 K, magnetic field 0.1 T in the plane of the sample. (e) dI/dV(V) spectrum of an *oxygen-down* molecule (red curve) and spectrum of the bare Pb (blue curve). Experimental conditions same as in (d).

Available as *Nano Lett.* 2018, 18, 12, 7955–7961 https://doi.org/10.1021/acs.nanolett.8b03921

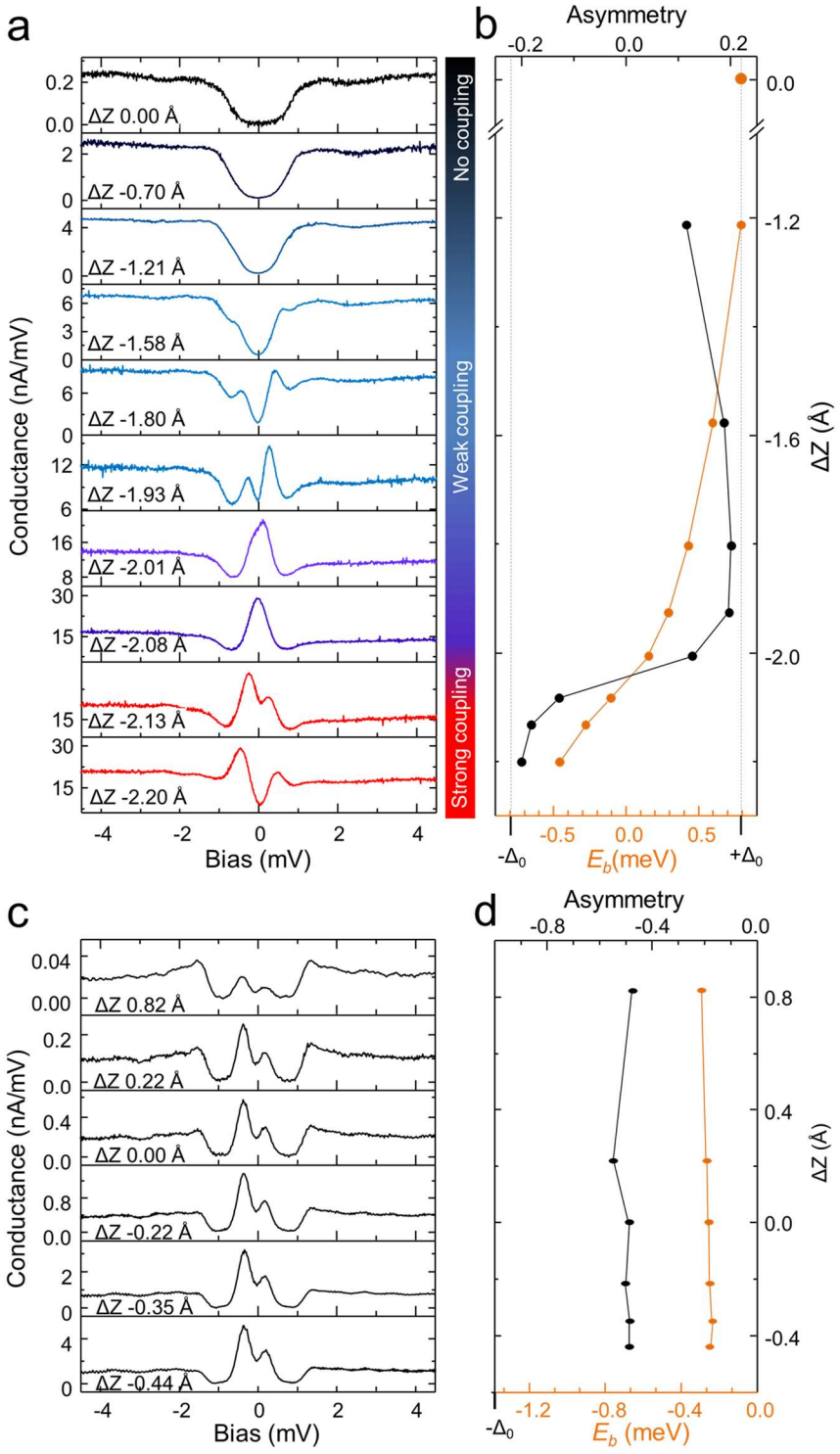

Figure 3. Mechanical interaction with STM tip. (a) dI/dV(V) spectra of an *oxygen-up* molecule recorded at different tip-sample distances. Line colors indicate the different coupling regimes as illustrated by the color bar on the right. (b) The YSR bound state energy (E_b) and peak asymmetry

for *oxygen-up* molecules obtained by fitting the spectra in (a) (see SI for details on fit routine). In the weak coupling range the peak at $V > 0$ has higher amplitude and $E_b > 0$ and in the strong coupling regime the higher amplitude peak is at V < 0 and $E_b < 0$. Peak asymmetry was calculated as $(A^+ - A^-)/(A^+ + A^-)$ where A^+ (A^-) is the area of the peak at $+E_b$/e ($-E_b$/e). (c) dI/dV(V) spectra of an *oxygen-down* molecule recorded at different tip-sample distances. (d) The YSR bound state energy (E_b) and the peak asymmetries for oxygen-down molecules obtained by fitting the spectra in (c). Temperature was 0.5 K and magnetic field 0.1 T for all measurements. Tunnel junction setpoint 5.0 mV, 1.0 nA was chosen as ΔZ = 0 Å.

Available as *Nano Lett.* 2018, 18, 12, 7955–7961 https://doi.org/10.1021/acs.nanolett.8b03921

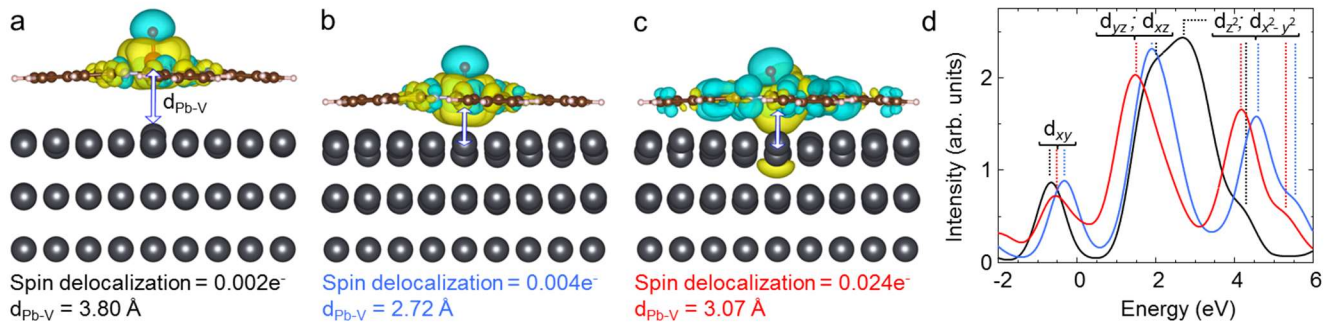

Figure 4. DFT calculations for *oxygen-up* VOPc on Pb. (a) Ball-and-stick model of oxygen-up VOPc (small balls) on the Pb surface (big balls, three layers shown). Isosurfaces of the spin density (yellow: spin up, cyan: spin down) illustrate the varying spin delocalization for (a) optimized geometry of the unperturbed molecule, (b) compressed VOPc and (c) compressed VOPc with additional tilt of VO by 30 ° toward the Pc plane. Pb surface to V distance, d_{Pb-V}, and amount of spin delocalization into first Pb layer stated below each panel. The isosurface level was set to 10^{-4} electrons per unit cell. (d) Vanadium 3d projected density of states, pDOS, calculated for the three structures (black: (a), blue: (b), red: (c)).

Available as *Nano Lett.* 2018, 18, 12, 7955–7961 https://doi.org/10.1021/acs.nanolett.8b03921

Table 1. Spin delocalization (e^-) calculated for the optimized geometries of the *oxygen-up* and *oxygen-down* geometries on different adsorption sites.

oxygen-up			
	Pb(111) Top layer	**V**	**O**
Top	-0.0019	1.18	-0.14
Hollow	-0.0012	1.18	-0.14
Bridge	-0.0010	1.18	-0.14
oxygen-down			
	Pb(111) Top layer	**V**	**O**
Top	0.014	1.18	-0.11
Hollow	0.025	1.19	-0.11

Table 2. Spin delocalization (e^-) calculated for the optimized geometry of the *oxygen-up* (top adsorption site) geometry and under different mechanical perturbation by the STM tip.

***oxygen*-up**				
V-Pb(111) distance (Å)	**V=O rotation induced**	**Pb(111) Top layer**	**V**	**O**
3.55 (optimized)	-	-0.0019	1.18	-0.14
2.72	-	-0.0043	1.16	-015
3.07	30 °	0.0237	1.04	-0.17

ASSOCIATED CONTENT

Preparation details of VOPc on Pb(111) islands grown on Si(111);

Preparation of VOPc on a Pb(111) single crystal;

Computational methods;

VOPc adsorption sites;

XPS characterization of the VOPc deposited on a Pb(111) single crystal;

XNLD characterization of VOPc deposited on a Pb(111) single crystal;

XMCD characterization of VOPc deposited on Pb(111) at 4.2 K;

Simulation of the magnetization curves;

XMCD characterization of the VOPc bulk reference;

MnPc adsorption sites;

Fit procedure for the dI/dV(V) spectra;

Spin delocalization VOPc-Pb(111) distance dependence;

This material is available free of charge via the Internet at http://pubs.acs.org

Corresponding Author

*(SL) E-mail: sebastian.loth@fmq.uni-stuttgart.de

*(LM) E-mail: luigi.malavolti@fmq.uni-stuttgart.de

Available as *Nano Lett.* 2018, 18, 12, 7955–7961 https://doi.org/10.1021/acs.nanolett.8b03921

Author Contributions

The manuscript was written through contributions of all authors. All authors have given approval to the final version of the manuscript.

Funding Sources

The research leading to these results has received funding from the European Research Council (ERC-2014-StG-633818-dasQ). Support from European COST Action CA15128 MOLSPIN and the Quantera ERA-NET Co-fund project SUMO are acknowledged. Italian MIUR, through PRIN project QCNaMoS (2015-HYFSRT), and Fondazione Ente Cassa di Risparmio di Firenze are acknowledged for financial support.

ACKNOWLEDGMENT

The authors thank K. Franke for fruitful discussions and E. Weckert and H. Dosch (Deutsches Elektronen-Synchrotron, Germany) for providing laboratory space. The research leading to these results has received funding from the European Research Council (ERC-2014-StG-633818-dasQ). Support from European COST Action CA15128 MOLSPIN and the Quantera ERA-NET Co-fund project SUMO are acknowledged. Italian MIUR, through PRIN project QCNaMoS (2015-HYFSRT), and Fondazione Ente Cassa di Risparmio di Firenze are acknowledged for financial support.

(1) Kubo, Y.; Ong, F. R.; Bertet, P.; Vion, D.; Jacques, V.; Zheng, D.; Dréau, A.; Roch, J.-F.; Auffeves, A.; Jelezko, F.; Wrachtrup, J.; Barthe, M. F.; Bergonzo, P.; Esteve, D. *Phys. Rev. Lett.* **2010**, *105* (14), 140502.

(2) Verdú, J.; Zoubi, H.; Koller, C.; Majer, J.; Ritsch, H.; Schmiedmayer, J. *Phys. Rev. Lett.* **2009**, *103* (4), 043603.

(3) Probst, S.; Rotzinger, H.; Wünsch, S.; Jung, P.; Jerger, M.; Siegel, M.; Ustinov, A. V; Bushev, P. A. *Phys. Rev. Lett.* **2013**, *110* (15), 157001.

(4) Bienfait, A.; Campagne-Ibarcq, P.; Kiilerich, A. H.; Zhou, X.; Probst, S.; Pla, J. J.; Schenkel, T.; Vion, D.; Esteve, D.; Morton, J. J. L.; Moelmer, K.; Bertet, P. *Phys. Rev. X* **2017**, *7* (4), 041011.

(5) Jenkins, M. D.; Zueco, D.; Roubeau, O.; Aromí, G.; Majer, J.; Luis, F. *Dalt. Trans.* **2016**, *45* (42), 16682–16693.

(6) Pientka, F.; Glazman, L. I.; von Oppen, F. *Phys. Rev. B* **2013**, *88* (15), 155420.

(7) Nadj-Perge, S.; Drozdov, I. K.; Li, J.; Chen, H.; Jeon, S.; Seo, J.; MacDonald, A. H.; Bernevig, B. A.; Yazdani, A. *Science* **2014**, *346* (6209), 602–607.

(8) Kim, H.; Palacio-Morales, A.; Posske, T.; Rózsa, L.; Palotás, K.; Szunyogh, L.; Thorwart, M.; Wiesendanger, R. *Sci. Adv.* **2018**, *4* (5), 1–8.

(9) Kamlapure, A.; Cornils, L.; Wiebe, J.; Wiesendanger, R. *Nat. Commun.* **2018**, *9* (1), 3253.

(10) Peng, Y.; Pientka, F.; Glazman, L. I.; Von Oppen, F. *Phys. Rev. Lett.* **2015**, *114* (10), 1–5.

(11) Sarma, S. Das; Freedman, M.; Nayak, C. *npj Quantum Inf.* **2015**, *1* (1), 15001.

(12) Yu, L. *Acta Phys. Sin.* **1965**, *21*, 75–91.

(13) Shiba, H. *Prog. Theor. Phys.* **1968**, *40* (3), 435.

(14) Rusinov, A. I. *Sov. J. Exp. Theor. Phys.* **1969**, *29* (6), 1101.

(15) Franke, K. J.; Schulze, G.; Pascual, J. I. *Science* **2011**, *332* (6032), 940–944.

(16) Heinrich, B. W.; Pascual, J. I.; Franke, K. J. *Prog. Surf. Sci.* **2018**, *93* (1), 1–19.

(17) Yazdani; Jones; Lutz; Crommie; Eigler. *Science* **1997**, *275* (5307), 1767–1770.

(18) Ji, S.-H.; Zhang, T.; Fu, Y.-S.; Chen, X.; Ma, X.-C.; Li, J.; Duan, W.-H.; Jia, J.-F.; Xue, Q.-K. *Phys. Rev. Lett.* **2008**, *100* (22), 226801.

(19) Ménard, G. C.; Guissart, S.; Brun, C.; Pons, S.; Stolyarov, V. S.; Debontridder, F.; Leclerc, M. V.; Janod, E.; Cario, L.; Roditchev, D.; Simon, P.; Cren, T. *Nat. Phys.* **2015**, *11* (12), 1013–1016.

(20) Ruby, M.; Pientka, F.; Peng, Y.; von Oppen, F.; Heinrich, B. W.; Franke, K. J. *Phys. Rev. Lett.* **2015**, *115* (8), 087001.

(21) Heinrich, B. W.; Braun, L.; Pascual, J. I.; Franke, K. J. *Nat. Phys.* **2013**, *9* (12), 765–768.

(22) Hatter, N.; Heinrich, B. W.; Ruby, M.; Pascual, J. I.; Franke, K. J. *Nat. Commun.* **2015**, *6* (1), 8988.

(23) Kezilebieke, S.; Dvorak, M.; Ojanen, T.; Liljeroth, P. *Nano Lett.* **2018**, *18* (4), 2311–2315.

(24) Island, J. O.; Gaudenzi, R.; de Bruijckere, J.; Burzurí, E.; Franco, C.; Mas-Torrent, M.; Rovira, C.; Veciana, J.; Klapwijk, T. M.; Aguado, R.; van der Zant, H. S. J. *Phys. Rev. Lett.*

2017, *118* (11), 117001.

(25) Etzkorn, M.; Eltschka, M.; Jäck, B.; Ast, C. R.; Kern, K. *arXiv:1807.00646* **2018**.

(26) Yoshizawa, S.; Minamitani, E.; Vijayaraghavan, S.; Mishra, P.; Takagi, Y.; Yokoyama, T.; Oba, H.; Nitta, J.; Sakamoto, K.; Watanabe, S.; Nakayama, T.; Uchihashi, T. *Nano Lett.* **2017**, *17* (4), 2287–2293.

(27) Farinacci, L.; Ahmadi, G.; Reecht, G.; Ruby, M.; Bogdanoff, N.; Peters, O.; Heinrich, B. W.; von Oppen, F.; Franke, K. J. *arXiv:1807.01344* **2018**.

(28) Flatté, M. E.; Byers, J. M. *Phys. Rev. Lett.* **1997**, *78* (19), 3761–3764.

(29) Atzori, M.; Tesi, L.; Morra, E.; Chiesa, M.; Sorace, L.; Sessoli, R. *J. Am. Chem. Soc.* **2016**, *138* (7), 2154–2157.

(30) Bonizzoni, C.; Ghirri, A.; Atzori, M.; Sorace, L.; Sessoli, R.; Affronte, M. *Sci. Rep.* **2017**, *7* (1), 1–8.

(31) Atzori, M.; Chiesa, A.; Morra, E.; Chiesa, M.; Sorace, L.; Carretta, S.; Sessoli, R. *Chem. Sci.* **2018**, *9* (29), 6183–6192.

(32) Eguchi, K.; Takagi, Y.; Nakagawa, T.; Yokoyama, T. *J. Phys. Chem. C* **2013**, *117* (44), 22843–22851.

(33) Zhang, J.; Wang, Z.; Niu, T.; Li, Z.; Chen, W. *Appl. Phys. Lett.* **2014**, *104* (11), 113506.

(34) Niu, T.; Zhang, J.; Chen, W. *J. Phys. Chem. C* **2014**, *118* (8), 4151–4159.

(35) Leijnse, M.; Flensberg, K. *Phys. Rev. Lett.* **2013**, *111* (6), 1–5.

(36) Chang, S. H.; Su, W. B.; Jian, W. B.; Chang, C. S.; Chen, L. J.; Tsong, T. T. *Phys. Rev. B* **2002**, *66* (3), 039901.

(37) Rolf-Pissarczyk, S.; Burgess, J. A. J.; Yan, S.; Loth, S. *Phys. Rev. B* **2016**, *94* (22), 224504.

(38) Eguchi, K.; Takagi, Y.; Nakagawa, T.; Yokoyama, T. *J. Phys. Chem. C* **2014**, *118* (31), 17633–17637.

(39) Grill, L.; Rieder, K.-H.; Moresco, F.; Stojkovic, S.; Gourdon, A.; Joachim, C. *Nano Lett.* **2006**, *6* (12), 2685–2689.

(40) Burgess, J. A. J.; Malavolti, L.; Lanzilotto, V.; Mannini, M.; Yan, S.; Ninova, S.; Totti, F.; Rolf-Pissarczyk, S.; Cornia, A.; Sessoli, R.; Loth, S. *Nat Commun* **2015**, *6*.

(41) Sonntag, A.; Hermenau, J.; Schlenhoff, A.; Friedlein, J.; Krause, S.; Wiesendanger, R. *Phys. Rev. Lett.* **2014**, *112* (1), 017204.

(42) Hsu, P.-J.; Kubetzka, A.; Finco, A.; Romming, N.; von Bergmann, K.; Wiesendanger, R. *Nat. Nanotechnol.* **2016**, *12* (2), 123–126.

(43) Yan, S.; Choi, D.-J.; Burgess, J. A. J.; Rolf-Pissarczyk, S.; Loth, S. *Nat. Nanotechnol.* **2014**, *10* (1), 40–45.

(44) Hiraoka, R.; Minamitani, E.; Arafune, R.; Tsukahara, N.; Watanabe, S.; Kawai, M.; Takagi, N. *Nat. Commun.* **2017**, *8* (May), 16012.

(45) Ternes, M.; Lutz, C. P.; Hirjibehedin, C. F.; Giessibl, F. J.; Heinrich, A. J. *Science* **2008**, *319* (5866), 1066–1069.

(46) Jacob, D.; Soriano, M.; Palacios, J. J. *Phys. Rev. B* **2013**, *88* (13), 134417.

Available as *Nano Lett.* 2018, 18, 12, 7955–7961 https://doi.org/10.1021/acs.nanolett.8b03921

Available as *Nano Lett.* 2018, 18, 12, 7955–7961 https://doi.org/10.1021/acs.nanolett.8b03921

Insert Table of Contents Graphic and Synopsis Here